

## QCD ON ANISOTROPIC LATTICES

G. BURGERS and F. KARSCH

*CERN, Geneva, Switzerland*

A. NAKAMURA

*Freie Universität, Berlin, FRG*

I.O. STAMATESCU

*MPI, München and Freie Universität, Berlin, FRG.*

Received 26 October 1987

We study the formulation of QCD on anisotropic lattices with different couplings in space and time directions of a four-dimensional hypercube. A non-perturbative determination of the ratio of lattice spacings,  $\xi = a_0/a_\tau$ , as well as the ratio of  $\Lambda$ -parameters has been performed in the scaling regime of SU(3) gauge theory. We apply these results to the thermodynamics of QCD on anisotropic lattices.

### 1. Introduction

Most lattice simulations of QCD are performed on isotropic lattices, i.e. lattices with identical lattice spacings in the space and time directions. This is certainly the most natural approach for many problems. However, in particular the analysis of temperature effects on isotropic euclidean lattices is limited in several respects. The temperature is related to the time-like extent of the lattice through  $1/T = N_\tau a$ , where  $N_\tau$  denotes the number of lattice sites in this direction and  $a$  is the lattice spacing. Thus, the highest temperature one can reach on an isotropic lattice is limited by  $T_{\max} = 1/a$ . It has recently been observed that this is a severe limitation in the analysis of the SU(2) Higgs model where the symmetry-restoring phase transition seems to take place at temperatures which are of the order of  $a^{-1}$  [1, 2]. Clearly, having only one site in the time direction will also lead to large finite-size effects. Moreover, the introduction of an anisotropy, i.e. different lattice spacings in space and time directions, may help in this case.

Another problem of considerable interest is the calculation of spectral functions for QCD at finite temperature. This is relevant for the calculation of transport

coefficients in the QCD plasma phase [3] or for the temperature dependence of hadron masses [4]. This, however, requires the knowledge of thermal correlation functions at several Matsubara frequencies. The number of modes that can be determined is limited by  $N_\tau/2$ . Thus, introducing a smaller lattice spacing ( $a_\tau$ ) in the time direction than in the space direction ( $a$ ) allows us to introduce more sites in the time direction, while keeping the temperature  $T = (N_\tau a_\tau)^{-1}$  and the spatial cut-off fixed.

Anisotropic lattices have been used in the past to study various aspects of QCD [5–7]. For instance, it turns out that anisotropic lattices can be used to disentangle finite-temperature and bulk phase transitions in large  $N$   $SU(N)$  gauge models [6]. They also give additional information on the approach to asymptotic scaling in  $SU(N)$  models [7]. In all these numerical approaches the anisotropy  $\gamma = \sqrt{K_\sigma/K_\tau}$ ,  $K_\sigma(K_\tau)$  denoting the couplings for space-(time)-like plaquettes, has been interpreted as the ratio of lattice spacings, i.e.  $\gamma = a_\sigma/a_\tau$ . This, in fact, is the interpretation of  $\gamma$  in the naive continuum limit neglecting quantum corrections [8, 9]. It is the purpose of this paper to study these quantum corrections in more detail and show how the ratio of lattice spacings,  $\xi \equiv a_\sigma/a_\tau$ , can be extracted from measurements of physical observables on lattices with given anisotropy  $\gamma$ . This is important in order to keep control over the physical temperature which is related to  $\xi$  rather than the input parameter  $\gamma$ .

This paper is organized as follows. In sect. 2, we discuss the formulation of QCD on anisotropic lattices and summarize some perturbative results. Sect. 3 deals with a non-perturbative determination of the ratio of lattice spacings  $\xi$  and the ratio of  $\Lambda$  parameters  $\Lambda_\xi/\Lambda_1$  which characterize different regularization schemes. We show Monte Carlo results for  $SU(3)$ . In sect. 4, we discuss the thermodynamics on anisotropic lattices and present further Monte Carlo data for  $SU(2)$ . Sect. 5 contains our conclusions.

## 2. Anisotropic lattices

An anisotropy can be introduced into standard  $SU(N)$  lattice gauge theory by choosing different couplings for plaquette variables in different planes of a hypercubic lattice. We will restrict ourselves here to the special case of two different couplings, i.e., a coupling  $K_\sigma$  for space–space plaquettes and  $K_\tau$  for space–time plaquettes. The standard Wilson action for pure  $SU(N)$  lattice gauge theory reads then

$$S = K_\sigma \sum_{i>j \neq 0}^x P_{x,ij} + K_\tau \sum_{i \neq 0}^x P_{x,0i}, \quad (2.1)$$

with

$$P_{x,\mu\nu} = \frac{1}{2N} \text{Tr}(\mathbf{1} - U_{x,\mu} U_{x+\mu,\nu} U_{x+\nu,\mu}^+ U_{x,\nu}^+) + \text{h.c.} \quad (2.2)$$

Let us define two new couplings

$$\beta = \sqrt{K_\sigma K_\tau}, \quad \gamma = \sqrt{K_\tau / K_\sigma}, \tag{2.3}$$

in terms of which the action, eq. (2.1), becomes

$$S = \beta \left( \frac{1}{\gamma} \sum_{\substack{x \\ i > j \neq 0}} P_{x,ij} + \gamma \sum_{\substack{x \\ i \neq 0}} P_{x,0i} \right). \tag{2.4}$$

Thus, for  $\gamma = 1$  we have the standard isotropic lattice formulation, while  $\gamma \neq 1$  introduces an explicit anisotropy. In the naive continuum limit ( $\beta \rightarrow \infty$ ,  $\gamma$  fixed)  $\gamma$  has to be interpreted as the ratio of lattice spacings in space ( $a \equiv a_\sigma$ ) and time ( $a_\tau$ ) directions. For finite  $\beta$ , however, this is no longer true. In the weak-coupling limit a relation between  $\gamma$  and the ratio of lattice spacings,  $\xi \equiv a/a_\tau$ , can still be established [8, 9]

$$\gamma \equiv \xi \eta^{-1} \tag{2.5}$$

with

$$\eta = 1 + N(c_\sigma(\xi) - c_\tau(\xi))/\beta + O(\beta^{-2}). \tag{2.6}$$

The functions  $c_\sigma(\xi)$ ,  $c_\tau(\xi)$  are given in ref. [9]. At intermediate couplings, however, the relation between  $\gamma$  and  $\xi$  is, a priori, unknown and has to be determined non-perturbatively, for instance, by checking rotational invariance on the anisotropic lattice [9]. We will explore this in sect. 4 in order to extract  $\eta$  from Wilson loop measurements.

When comparing physical observables calculated on lattices with different anisotropy  $\gamma$ , one has to take into account that the  $\Lambda$  parameters depend on these different regularization prescriptions [8, 9]

$$a\Lambda_\xi = \left( \frac{11N}{8\pi^2\beta} \right)^{-51/121} \exp \left\{ - \frac{4\pi^2}{11N} \beta \right\}, \tag{2.7}$$

$$\Lambda_\xi/\Lambda_1 = \exp \left\{ - \frac{12\pi^2}{11N} (c_\tau(\xi) + c_\sigma(\xi)) \right\}. \tag{2.8}$$

In an actual Monte Carlo simulation we calculate dimensionless observables, i.e. physical, dimensional quantities in units of the lattice cut-offs, as functions of  $\beta$  and  $\gamma$ . In the validity regime of eqs. (2.5)–(2.8), we can extract the corresponding dimensional quantities and express them in terms of a unique scale  $\Lambda_1$ . In general, however, this requires the knowledge of  $\eta$  as well as the ratio  $\Lambda_\xi/\Lambda_1$ , which may

both depend on  $\gamma$  and  $\beta^*$ . For given  $\gamma$  and  $\beta$ , we can determine  $\eta$  and  $\Lambda_\xi/\Lambda_1$  by comparing two physical quantities with corresponding measurements on an isotropic lattice. This will be used in the following to calculate  $\eta$  and  $\Lambda_\xi/\Lambda_1$  in the scaling regime of SU(3) gauge theory.

### 3. Non-perturbative determination of $\eta$ and $\Lambda_\xi/\Lambda_1$

In this section we perform a numerical analysis for the parameter  $\eta$  and  $\Lambda_\xi$  appearing in eqs. (2.5) and (2.7). We do this for the gauge group SU(3) because violations of asymptotic scaling are known to be large in this case [11]. We therefore expect sizable deviations from the weak-coupling results for  $\eta$  and  $\Lambda_\xi/\Lambda_1$  reviewed in sect. 2 as long as the asymptotic scaling regime has not been reached, i.e. for  $\beta \leq 6.0$ .

First we will discuss a determination of  $\eta(\beta, \gamma)$  from Wilson loop measurements [9]. We measure space-space ( $W_{\sigma\sigma}$ )- and space-time ( $W_{\sigma\tau}$ )- like Wilson loops of size  $n_1 \times n_2^{(\sigma)}$  and  $n_1 \times n_2^{(\tau)}$ , respectively. We parametrize the results in terms of a universal function  $f(x, y)$  and arbitrary normalization factors  $c_{\sigma\sigma}$  and  $c_{\sigma\tau}$ , i.e.

$$\begin{aligned} W_{\sigma\sigma}(n_1, n_2^{(\sigma)}) &= c_{\sigma\sigma} \exp\{f(n_1 a, n_2^{(\sigma)} a)\}, \\ W_{\sigma\tau}(n_1, n_2^{(\tau)}) &= c_{\sigma\tau} \exp\{f(n_1 a, n_2^{(\tau)} a)\}. \end{aligned} \quad (3.1)$$

If rotational symmetry is restored,  $V(x) = -\lim_{y \rightarrow \infty} (1/y) f(x, y)$  gives the heavy quark potential which has to be independent of the anisotropy<sup>\*\*</sup>. This motivates the above ansatz. Thus, if we know  $\xi = a/a_\tau$ , it should be possible to match all  $W_{\sigma\sigma}$  and  $W_{\sigma\tau}$  data up to an overall normalization

$$W_{\sigma\tau}(n_1, n_2^{(\tau)} = \xi n_2^{(\sigma)}) = \frac{c_{\sigma\tau}}{c_{\sigma\sigma}} W_{\sigma\sigma}(n_1, n_2^{(\sigma)}). \quad (3.2)$$

For a given anisotropy  $\gamma$  we then find  $\eta$  from eq. (2.5) as

$$\eta = \gamma^{-1} \frac{n_2^{(\tau)}}{n_2^{(\sigma)}}, \quad (3.3)$$

with  $n_2^{(\tau)}, n_2^{(\sigma)}$  being those values for which the matching condition eq. (3.2) holds.

\* In principle, they can also depend on  $N_\sigma, N_\tau$ . However, we will ignore these finite-size effects in the following discussion. For free Bose and Fermi systems these effects have been analyzed in ref. [10].

\*\* In some cases we performed simulations on lattices which are not completely symmetric, i.e.  $N_\sigma \neq \gamma N_\tau$ . These finite-size effects for the potential, however, are small as long as we stay in the confined phase.

We have calculated Wilson loops on  $8^3 \times N_\tau$ ,  $N_\tau = 4, \dots, 16$  lattices for various anisotropies  $\gamma$  and  $\beta$ -values ( $5.55 \leq \beta \leq 5.75$ ). We used a standard Metropolis algorithm. In fig. 1a, we show the two sets of Wilson loops for the  $8^3 \times 16$  lattice at  $\beta = 5.65$  and  $\gamma = 2$ . The data are plotted on a double logarithmic scale. The scale of the space–space loops has been “rescaled” relative to that for space–time loops according to eq. (3.3), assuming  $\eta = 1$ . Apparently, the two sets of Wilson loops do not match with this assumption. Note that varying the free parameter  $c_{\sigma\tau}/c_{\sigma\sigma}$  corresponds to a shift of the vertical scale while a shift of the horizontal scale corresponds to a change of  $\eta$ . In fig. 1b, we show the same data replotted using  $\eta = 1.32$ . A good agreement between both sets of Wilson loops can now be found for all  $n_1, n_2$  values. The value required for  $c_{\sigma\sigma}/c_{\sigma\tau}$  deviates only a little from 1; this turns out to be true also in the rest of the cases, but as we are not interested in the value of  $c_{\sigma\tau}/c_{\sigma\sigma}$ , we shall not mention its value in the following.

In fig. 1c, we show results at  $\beta = 5.7$ ,  $\gamma = 2$ . The “best fit” for  $\eta$  gives  $\eta = 1.29$ . The “best fit” for  $\eta$  is done by eye, shifting the double logarithmic plots. A real fit would imply an interpolation assumption for the various  $n_1, n_2$  values and therefore it would be only more objective in appearance. In fig. 2 we show data on a simply logarithmic scale, to illustrate again the rescaling equation (3.2) and at the same time to show that no simple  $n_1, n_2$  dependence can be found which could be used for an objective fit. The results are given in table 1. The errors quoted are estimated on the basis of the errors for the Wilson loops. They are very subjective but we consider them as rather conservative. From table 1, we see that in our small range of  $\beta$  values we could not detect a systematic  $\beta$ -dependence of  $\eta$ . The measured values for  $\eta$  are considerably larger than predicted on the basis of the perturbative relation, eq. (2.6).

In order to compare physical quantities calculated on lattices with different anisotropy  $\gamma$ , it is necessary to know the ratio of scale parameters  $\Lambda_\xi/\Lambda_1$  for these different regularizations. In the asymptotic scaling regime this ratio will be a  $\beta$ -independent function of  $\xi$  which has been calculated in perturbation theory [eq. (2.8)]. However, we know that for  $\beta < 6$ , violations of asymptotic scaling are large [11]. Assuming the validity of the RG equation, eq. (2.7), these scaling violations may be parametrized by a  $\beta$ -dependent  $\Lambda$  parameter. First calculations by Thacker and Sexton [7] on anisotropic lattices, however, seem to indicate that also below  $\beta = 6$ , the ratio  $\Lambda_\xi/\Lambda_1$  follows the perturbative prediction despite the apparent violations of asymptotic scaling\*.

Knowing the value  $\eta$  from our Wilson loop measurements, we can determine the ratio  $\Lambda_\xi/\Lambda_1$  by demanding that an observable measured on lattices with  $\gamma = 1$  and  $\gamma \neq 1$ , respectively, yields the same physical value independent of the regularization scheme used. We have chosen the deconfinement temperature as an observable to

\* Note that Thacker and Sexton use a somewhat different approach. They introduce an anisotropy in one of the space directions. This way they did not have to determine  $\eta$ .

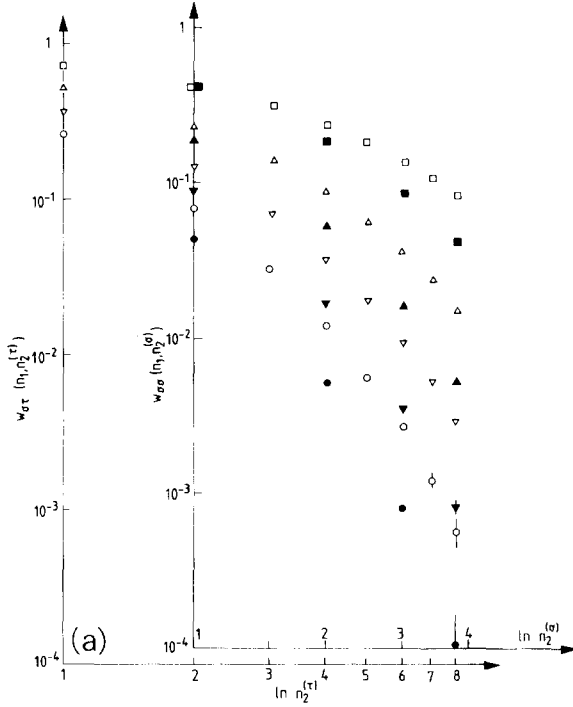


Fig. 1. Double logarithmic plots for Wilson loops.  $W_{\sigma\tau}(n_1, n_2^{(\tau)})$  – empty symbols – and  $W_{\sigma\sigma}(n_1, n_2^{(\sigma)})$  – full symbols – are plotted versus  $n_2^{(\tau)}$ ,  $n_2^{(\sigma)}$ , respectively. Here,  $n_1 = 1$  ( $\square, \blacksquare$ ), 2 ( $\triangle, \blacktriangle$ ), 3 ( $\nabla, \blacktriangledown$ ) and 4 ( $\circ, \bullet$ ). To indicate the shifts we give both pairs of co-ordinate axes. The lattice size is  $8^3 \times 16$ . (a)  $\beta = 5.65$ ,  $\gamma = 2$ . The data are plotted shifted according to  $\eta = 1$ . (b) Same data, replotted shifted according to the “best fit”  $\eta = 1.32$ . (c)  $\beta = 5.70$ ,  $\gamma = 2$ . The data are plotted shifted according to the “best fit”  $\eta = 1.29$ .

extract  $\Lambda_\xi/\Lambda_1$  from MC simulations. We determine the critical couplings  $\beta_c^1$  and  $\beta_c^\xi$  on a lattice with  $\gamma = 1$  and  $N_\tau^1$  sites in the time direction and  $\gamma \neq 1$  and  $N_\tau^\xi$  sites, respectively.  $N_\tau^\xi$  has been chosen such that  $N_\tau^\xi = \gamma N_\tau^1$ . From eq. (2.7) we find then for the critical temperatures

$$\begin{aligned} \gamma = 1: \quad & \frac{\Lambda_1}{T_1} = N_\tau^1 R(\beta_c^1), \\ \gamma \neq 1: \quad & \frac{\Lambda_\xi}{T_\xi} = \left( \frac{N_\tau^\xi}{\gamma} \right) \eta^{-1} R(\beta_c^\xi). \end{aligned} \quad (3.4)$$

Demanding that the critical temperatures are  $\gamma$ -independent we find

$$\frac{\Lambda_\xi}{\Lambda_1} = \eta^{-1} \frac{R(\beta_c^\xi)}{R(\beta_c^1)}. \quad (3.5)$$

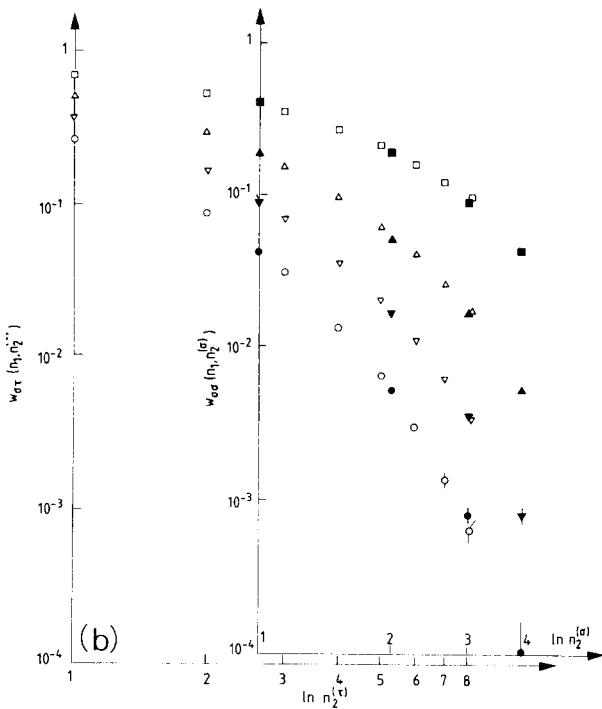
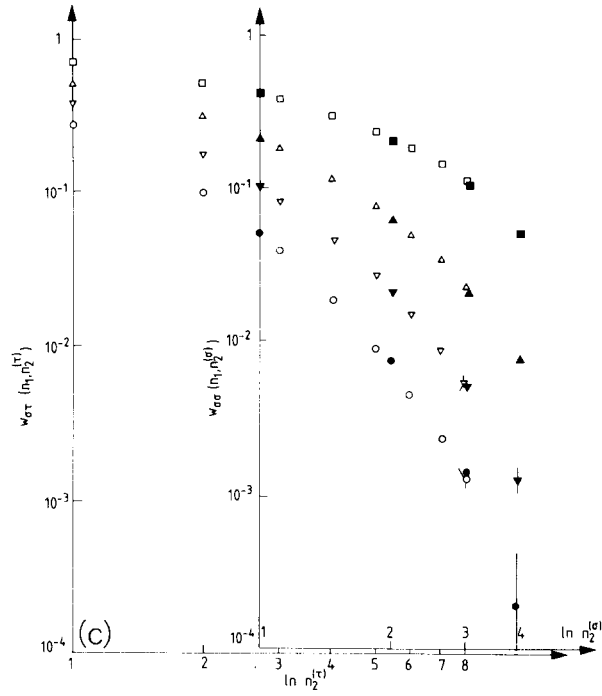


Fig. 1. (continued.)

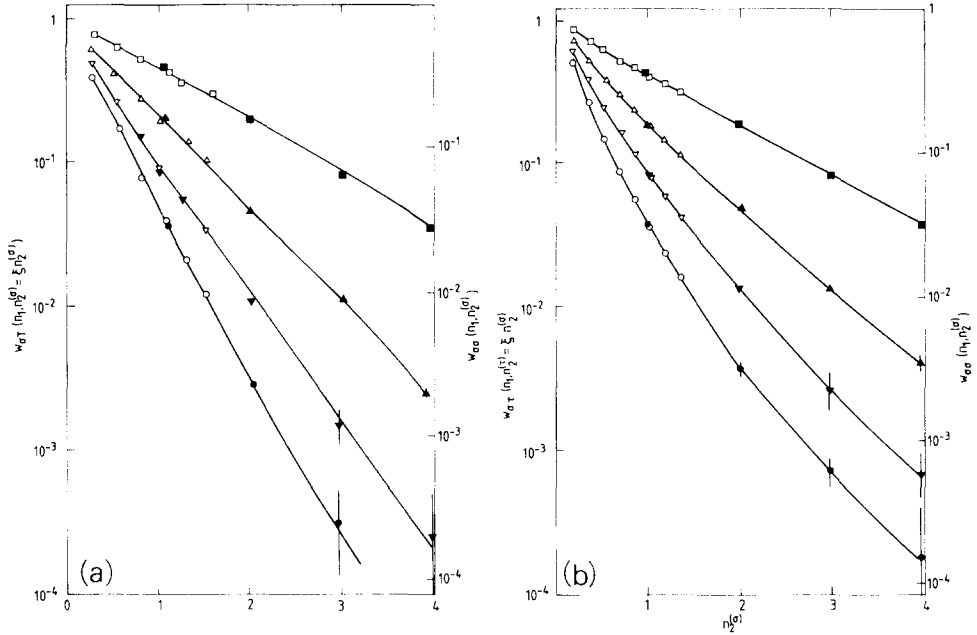


Fig. 2. Simply logarithmic plots for Wilson loops versus  $n_2^{(\sigma)}$  (same symbols as in fig. 1). (a)  $8^3 \times 12$  lattice,  $\beta = 5.55$ ,  $\gamma = 3$ . The  $W_{\sigma T}$  points are plotted and rescaled according to the “best fit”  $\eta = 1.39$ . (b)  $8^3 \times 16$  lattice,  $\beta = 5.55$ ,  $\gamma = 4$ . The  $W_{\sigma T}$  points are plotted and rescaled according to the “best fit”  $\eta = 1.54$ . The lines connecting the points are only meant to guide the eye and to indicate the deviations from a linear dependence.

TABLE I  
Values of  $\eta$  obtained by Wilson loop analysis. All the results are obtained in the confined phase

$\gamma$	Lattice	$\beta$	$\eta$
1.05	$8^3 \times 12$	5.70	$1.02 \pm 0.03$
1.1	$8^3 \times 12$	5.66	$1.03 \pm 0.03$
		5.68	$1.05 \pm 0.05$
		5.70	$1.07 \pm 0.04$
		5.72	$1.05 \pm 0.05$
		5.70	$1.32 \pm 0.07$
2.0	$8^3 \times 12$	5.65	$1.32 \pm 0.05$
	$8^3 \times 16$	5.70	$1.29 \pm 0.05$
		5.75	$1.31 \pm 0.07$
2.2	$8^3 \times 16$	5.70	$1.39 \pm 0.07$
2.5	$8^3 \times 12$	5.70	$1.43 \pm 0.06$
3.0	$8^3 \times 12$	5.55	$1.39 \pm 0.08$
			$-0.05$
4.0	$8^3 \times 16$	5.55	$1.54 \pm 0.07$



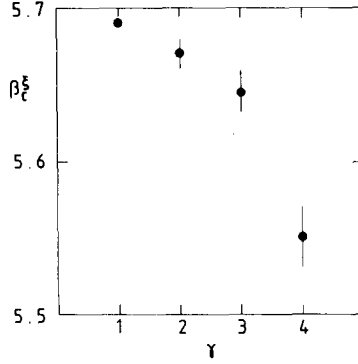


Fig. 3.  $\beta_c^\xi$  as a function of  $\gamma$  on lattices  $8^3 \times N_\tau$  with  $N_\tau = 4\gamma$ . The large errors are due to strong metastabilities in the phase transition region.

TABLE 2

$\Lambda_\xi/\Lambda_1$  obtained from the critical couplings for the deconfinement temperature (last column) using eq. (4.5). Also given is the perturbative result from eq. (2.8). The value of  $\eta$  is taken from table 1.

The resulting value for the ratio of lattice spacings is displayed in the fourth column

$N_\tau$	$\gamma$	$\eta$	$\xi = \eta\gamma$	$\beta_c$	$\Lambda_\xi/\Lambda_1$ (pert.)	$\Lambda_\xi/\Lambda_1$ (MC)
4	1	1	1	$5.689 \pm 0.002$	1	1
8	2	$1.31 \pm 0.03$	$2.62 \pm 0.12$	$5.67 \pm 0.01$	0.815	$0.78 \pm 0.02$
12	3	$1.39 \pm 0.07$	$4.17 \pm 0.21$	$5.645 \pm 0.015$	0.799	$0.76 \pm 0.04$
16	4	$1.54 \pm 0.07$	$6.16 \pm 0.28$	$5.55 \pm 0.02$	0.813	$0.77 \pm 0.04$

Note that eq. (3.5) defines lines of constant temperature in the  $\beta$ - $\gamma$  coupling plane. Lines at constant spatial cut-off  $a$  are given by eq. (3.5) with  $\eta \equiv 1$ . In fig. 3 we show results for the critical couplings  $\beta_c^\xi$  obtained from simulations on  $8^3 \times N_\tau$  lattices with  $N_\tau/\gamma = 4$  and  $\gamma = 1, 2, 3, 4$ . As can be seen, the critical coupling gets shifted to smaller values. Using the values for  $\eta$  from table 1 and the measured critical couplings  $\beta_c^\xi$ , we can obtain  $\Lambda_\xi/\Lambda_1$  from eq. (3.5). The results are given in table 2. Indeed, the measured values for  $\Lambda_\xi/\Lambda_1$  agree rather well with the perturbative prediction which is given in the last column of table 2. This indicates that asymptotic-scaling violations are indeed to a large extent independent of  $\gamma$  [7], although we find systematically lower values than predicted by weak-coupling perturbation theory. Our results for  $\eta$  and  $\Lambda_\xi/\Lambda_1$  are summarized in figs. 4 and 5. Here we also show the weak-coupling predictions [9].

#### 4. Thermodynamics on anisotropic lattices

We want to illustrate how the discussion of the previous sections becomes relevant for the analysis of the thermodynamics of a gluon gas on anisotropic

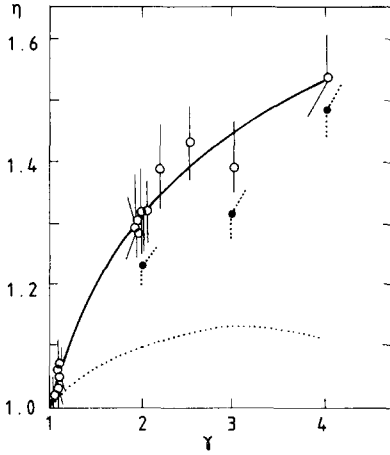


Fig. 4.  $\eta$  versus  $\gamma$  as determined from Wilson loops (table 1). For illustration we also show the  $\eta$ 's which we obtain from the critical temperature data using the perturbative ratio of  $\Lambda$ -parameters, eq. (2.8) – full points. The dotted line shows the weak-coupling (one-loop) result, eq. (2.6), for  $\beta$  values of  $5.65 \pm 0.10$ . The full line is a fit to the data;  $\eta = 1 + c(1/\sqrt{\gamma} - 1)$  with  $c = -1.069 \pm 0.060$ .

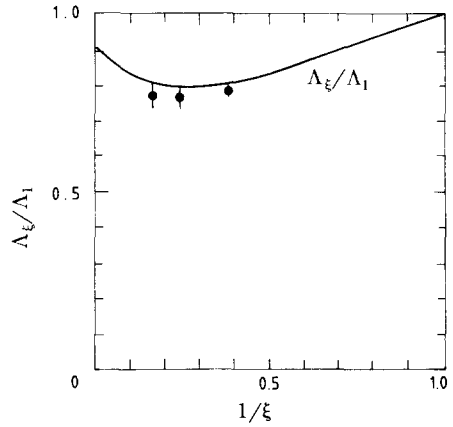


Fig. 5.  $\Lambda_\xi/\Lambda_1$  for SU(3). The points are taken from the numerical analysis (table 2, last column) at  $\gamma = 2, 3$  and 4. The curve represents  $\Lambda_\xi/\Lambda_1$  from eq. (2.8), the weak-coupling result to one loop. Notice that here the abscissa is  $\xi = \eta\gamma$ .

lattices. In particular, we will analyze the energy density calculated on anisotropic lattices and show that results consistent with standard calculations on isotropic lattices can be obtained. As mentioned before, the true advantage of the anisotropic formulation should show up in the calculation of thermal correlation functions [3, 4]. This will be discussed elsewhere.

We want to evaluate the energy density [10]

$$\varepsilon/T^4 = \left( \frac{N_\tau}{N_\sigma} \right)^3 \xi^{-2} \frac{\partial \ln Z}{\partial \xi} \Bigg|_{a \text{ fixed}}. \quad (4.1)$$

Using eqs. (2.4) and (2.5) we find

$$\varepsilon/T^4 = 3N_\tau^4 \beta \gamma^{-4} \eta^{-3} [\bar{P}_\sigma - \gamma^2 \bar{P}_\tau] - 3N_\tau^4 (\gamma \eta)^{-3} \left[ \frac{d\beta_\sigma}{d\xi} \Bigg|_{a \text{ fixed}} \bar{P}_\sigma + (\gamma \eta)^2 \frac{d\beta_\tau}{d\xi} \Bigg|_{a \text{ fixed}} \bar{P}_\tau \right], \quad (4.2)$$

where we have defined the space- and time-like couplings  $\beta_\sigma, \beta_\tau$ , as

$$\beta_\sigma = \beta\eta, \quad \beta_\tau = \beta/\eta \quad (4.3)$$

$\bar{P}_\sigma$  ( $\bar{P}_\tau$ ) denote space–space (space–time) plaquette expectation values, which we have normalized by subtracting the zero-temperature contribution

$$\bar{P}_{\sigma(\tau)} = \langle P_{\sigma(\tau)} \rangle_{N_\tau < N_\sigma\gamma} - \langle P_{\sigma(\tau)} \rangle_{N_\tau = N_\sigma\gamma}. \quad (4.4)$$

Here the zero-temperature lattice has been approximated by a lattice of size  $N_\sigma^3 \times N_\tau$ , with  $N_\tau \equiv \gamma N_\sigma$ . The energy density depends explicitly on the two couplings  $\beta$  and  $\gamma$ . However, in addition it involves  $\eta$  and the derivatives of  $\beta_\sigma$  and  $\beta_\tau$  with respect to  $\xi$ . Some care has to be taken as these derivatives have to be evaluated along lines of constant  $a$ , i.e. by varying  $\xi$ , we have to change  $\beta$  according to eq. (3.5) with  $\eta \equiv 1^*$ . We thus have

$$\begin{aligned} \frac{d\beta_\sigma}{d\xi} &= \eta \frac{d\beta}{d\xi} + \beta\eta^{-1} \frac{d\eta}{d\gamma}, \\ \frac{d\beta_\tau}{d\xi} &= \eta \frac{d\beta}{d\xi} - \beta\eta^{-3} \frac{d\eta}{d\xi}, \end{aligned} \quad (4.5)$$

where we have used  $d\gamma/d\xi = \eta^{-1}$ . The derivative  $d\eta/d\gamma$  we extract from our measured  $\eta$ -values shown in fig. 4 and  $d\beta/d\xi$  from the  $\Lambda_\xi/\Lambda_1$  ratios. As the latter turned out to be close to the perturbative values, we have used the perturbative expression

$$\frac{d\beta}{d\xi} = 3(c_\sigma(\xi) + c_\tau(\xi)). \quad (4.6)$$

The derivative  $d\eta/d\gamma$  we got from a fit to our measured data. The resulting derivatives  $d\beta_{\sigma(\tau)}/d\xi$  are given in table 3. We note that these are about a factor 2–3 larger in magnitude than those which are perturbative. This is also important for simulations on isotropic lattices, where often the perturbative results for the derivatives are used in the scaling regime.

Let us finally discuss the thermodynamics of SU(2) gauge theory. In contrast to SU(3), we expect here that the perturbative relations for  $\eta$  and  $\Lambda_\xi/\Lambda_1$  hold in the whole scaling regime as scaling violations are known to be small for SU(2) above  $\beta \geq 2.1$  [13]. In fact, using the perturbative value for  $\eta$  and  $\partial\beta_{\sigma(\tau)}/\partial\xi$ , we find an energy density which is independent of the anisotropy. In fig. 6, we show  $\eta^3 \epsilon/T^4$  from a MC simulation on a  $8^3 \times N_\tau$  lattice with  $N_\tau$  and  $\gamma$  chosen such that

\* For a different approach to determine these derivatives non-perturbatively, see ref. [12].

TABLE 3

Derivatives of space- and time-like couplings defined in eq. (4.3). Columns 3 and 5 give perturbative results from ref. [9]. Columns 2 and 4 have been obtained from a fit to the data in fig. 4

$\xi$	$\partial\beta_g/\partial\xi$		$\partial\beta_\tau/\partial\xi$	
	MC	Weak coupl.	MC	Weak coupl.
1	$3.26 \pm 0.17$	1.21	$-2.84 \pm 0.17$	-0.79
2	$0.88 \pm 0.09$	0.33	$-0.42 \pm 0.09$	-0.18
3	$0.43 \pm 0.08$	0.12	$-0.21 \pm 0.08$	-0.10
4	$0.24 \pm 0.05$	0.06	$-0.10 \pm 0.05$	-0.07

$N_\tau/\xi = 2$ . The rise of  $\eta^3 \epsilon/T^4$  with increasing  $\gamma$  is obvious. This reflects the fact that  $\eta < 1$  for  $\gamma > 1$  and the factor  $\eta^3$  has still to be divided out to get the physical energy density  $\epsilon/T^4$ . Using  $\eta$  from eq. (2.6) we find  $\epsilon/T^4$  which is also shown in fig. 6. This is roughly  $\gamma$ -independent. In fact, the slight decrease of the data can be understood in terms of slightly different finite-size corrections for different  $\gamma$  [10]. Taking these corrections into account we get results indicated by crosses in fig. 6.

The data shown in fig. 6 have been obtained at fixed  $\beta$ . From the discussion in sects. 2 and 3 we know that this, in fact, corresponds to different temperatures, because with varying  $\gamma$  also the  $\Lambda$ -parameter changes in units of which the temperature is determined. The comparison in fig. 6 is insensitive to this as above  $T_c$ ,  $\epsilon/T^4$  is roughly constant. This is different in fig. 7 where we show the energy density on a  $8^3 \times 12$  lattice with anisotropy  $\gamma = 3$  and the Polyakov loop expectation value in a large temperature interval that includes the transition region. Here we

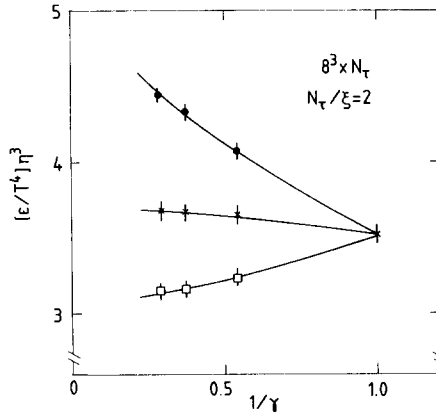


Fig. 6.  $\eta^3 \epsilon/T^4$  (dots) versus  $\gamma^{-1}$  for SU(2) on a  $8^3 \times N_\tau$  lattice at  $\beta = 2.2$ .  $N_\tau$  and  $\gamma$  have been chosen such that  $N_\tau/\xi = N_\tau \eta/\gamma = 2$ . Here the perturbative relation, eq. (2.6), has been used to determine  $\eta$ . Also shown is  $\epsilon/T^4$  (squares) and  $\epsilon/T^4 R(\gamma)$  (crosses) where  $R(\gamma)$  is a correction factor for finite-size effects [10] normalized to 1 for  $\gamma = 1$ .

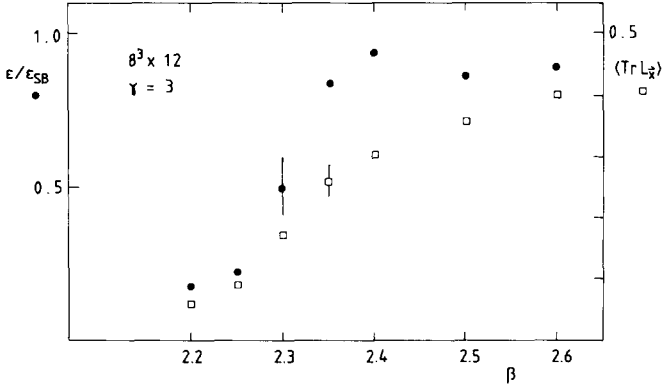


Fig. 7.  $\epsilon/\epsilon_{SB}$  versus  $T/\Lambda_1$  for SU(2) on a  $8^3 \times N_t$  lattice with  $N_t/\gamma = 4$ ,  $\gamma = 3$  (dots) and Polyakov loop expectation value (squares).

used the perturbative  $\eta$  values, eq. (2.6) and  $\Lambda_\xi/\Lambda_1$  ratio, eq. (2.8), to fix the temperature scale. We also took into account that finite-size effects on these small lattices are  $\xi$ -dependent [10]. Clearly, the overall behaviour is similar to the one found on isotropic lattices.

Thus, we see that for SU(2) the perturbative formulas for  $\eta$  and  $\Lambda_\xi/\Lambda_1$  hold well and identical results on anisotropic and isotropic lattices can be obtained.

## 5. Conclusions

We have analyzed the formulation of QCD on anisotropic lattices. We have shown that the naive interpretation of the anisotropy as ratio of space- and time-like lattice spacings does not hold in general. Quantum corrections ( $\eta > 1$ ) are important. Even in the regime where these corrections can be calculated perturbatively, they may lead to strong modifications; for instance, in the energy density these effects are clearly visible (see fig. 6).

We have shown that the ratio of lattice spacings as well as  $\Lambda_\xi/\Lambda_1$  can be determined non-perturbatively. In the scaling regime of SU(3) we find large deviations of  $\eta$  from the perturbative value while  $\Lambda_\xi/\Lambda_1$  agrees rather well with perturbation theory. The latter has been observed before [7] and indicates that violations of asymptotic scaling are to a large extent universal, i.e.  $\gamma$ -independent.

Although somewhat more computational effort is involved, we find that anisotropic lattices reproduce the physical results obtained from isotropic lattices. Moreover, they have the advantage that time resolution can be varied independently of the spatial resolution. This should make them more suitable for the determination of spectral functions [2, 3] and the simulation of very high temperatures at fixed spatial cut-off, as it is needed for the Higgs transition [1].

Part of the numerical calculations have been performed on the Cray-XMP of ZIB, Berlin.

### References

- [1] H.G. Evertz, J. Jersak and K. Kanaya, Nucl. Phys. B285 [FS19] (1987) 229
- [2] P.H. Damgaard and U.M. Heller, Santa Barbara preprint NSF-ITP-87-58 (1987)
- [3] F. Karsch and H.W. Wyld, Phys. Rev. D35 (1987) 2518
- [4] T. Hashimoto, O. Miyamura, K. Hirose and T. Kanki, Phys. Rev. Lett. 57 (1986) 2123
- [5] J. Kuti, J. Polonyi and K. Szlachanyi, Phys. Lett. B98 (1981) 199
- [6] S. Das and J.B. Kogut, Phys. Lett. B145 (1984) 375
- [7] S. Das and J.B. Kogut, Nucl. Phys. B265 [FS15] (1986) 303;  
J.C. Sexton and H.B. Thacker, Phys. Rev. Lett. 57 (1986) 2131
- [8] A. Hasenfratz and P. Hasenfratz, Nucl. Phys. B193 (1981) 210
- [9] F. Karsch, Nucl. Phys. B205 [FS5] (1982) 239
- [10] J. Engels, F. Karsch and H. Satz, Nucl. Phys. B205 [FS5] (1982) 239
- [11] K.C. Bowler, A. Hasenfratz, P. Hasenfratz, U. Heller, F. Karsch, R.D. Kenway, H. Meyer-Ortmanns, I. Montvay, G.S. Pawley and D.J. Wallace, Nucl. Phys. B257 [FS14] (1985) 155
- [12] I. Montvay and E. Pietarinen, Phys. Lett. B110 (1982) 148
- [13] P. Kackenzie, *in* Gauge theory on a lattice, eds. C. Zachos et al., Proc. ANL Workshop, Argonne National Laboratory, Argonne, 1984;  
U. Heller and F. Karsch, Phys. Rev. Lett. 54 (1985) 1765